Graphite First Wall Thermal Performance in ICF Reactors

H. Attaya, E. Lovell, R. Engelstad, R. Peterson, J. Liang, S. Abdel-Khalik, G. Moses and G. Kulcinski

April 1986

UWFDM-682

, Presented at the 2nd International Conference on Fusion Reactor Materials, 14-17 April 1986, Chicago, IL.

FUSION TECHNOLOGY INSTITUTE

UNIVERSITY OF WISCONSIN

MADISON WISCONSIN

Graphite First Wall Thermal Performance in ICF Reactors

H. Attaya, E. Lovell, R. Engelstad, R. Peterson, J. Liang, S. Abdel-Khalik, G. Moses and G. Kulcinski

Fusion Technology Institute
University of Wisconsin
1500 Engineering Drive
Madison, WI 53706

http://fti.neep.wisc.edu

April 1986

UWFDM-682

, Presented at the 2nd International Conference on Fusion Reactor Materials, 14-17 April 1986, Chicago, IL.

GRAPHITE FIRST WALL THERMAL PERFORMANCE IN ICF REACTORS

H. Attaya, E. Lovell, R. Engelstad,
R. Peterson, J. Liang, S. Abdel-Khalik,
G. Moses and G. Kulcinski

Fusion Technology Institute
University of Wisconsin
1500 Johnson Drive
Madison, WI 53706-1687

May 1986

Presented at the 2nd International Conference on
Fusion Reactor Materials, 14-17 April 1986, Chicago, IL

UWFDM-682

GRAPHITE FIRST WALL THERMAL PERFORMANCE IN ICF REACTORS

H. Attaya, E. Lovell, R. Engelstad, R. Peterson, J. Liang,
S. Abdel-Khalik, G. Moses, and G. Kulcinski

Fusion Technology Institute, Nuclear Engineering Department,
University of Wisconsin, 1500 Johnson Drive
Madison, WI 53706-1687 U.S.A.

Abstract

Graphite has been considered as a candidate material for the first wall in ICF reactors. This paper shows the thermal performance of the graphite first wall (GFW) in the 0.25 μm laser driven materials test reactor SIRIUS-M. The first wall temperature response due to the x-rays, reflected laser light, and ions that emanate from the 13.4 MJ yield target was calculated for dry GFWs which were either unprotected or gas protected (1 torr xenon). Evaporation rates and thermal stresses were calculated and minimum radii were chosen for both cases. It was found that the reflected laser light from the target produces the highest temperature rise in the gas protected GFW. If 10% of the laser light is reflected from the target and the reflectivity of graphite is 50%, the maximum thermal stress in the GFW is about 90% of the compressive strength for a 2 m radius cavity. Therefore, the viability of the first wall design depends critically on the laser light reflected from the target, the graphite reflectivity and the strength of the graphite.

1. Introduction

In ICF reactors utilizing dry first walls, the thermonuclear explosion energy is deposited in the first wall in a very short time. As a result, the temperature rise in the first wall is rather high. This makes it necessary to either use a large cavity with an unprotected wall, or utilize some form of wall protection. Use of an unprotected wall results in a low neutron wall loading which may be economically unattractive for power reactors. It is also unsuitable for materials test facilities which require a high wall loading in order to accomplish the facility mission in the shortest possible time. Use of "protected" high temperature materials for the first wall makes it possible to reach high neutron wall loadings at reasonably achievable repetition rates.

Graphite has been investigated and proposed [1,2] as a first wall material in ICF reactor designs. It has also been selected for use in the first dedicated ICF materials test facility SIRIUS-M [3]. In this paper we present the thermal and stress analyses for the GFW in SIRIUS-M with and without the use of xenon gas in the cavity. A more general review of SIRIUS-M can be found in these proceedings [4].

2. SIRIUS-M Radiation Spectra

SIRIUS-M uses single-shell targets that are illuminated uniformly by 1 MJ of KrF (0.248 μm) laser energy for about 11 ns. The target yield is 13.4 MJ partitioned as: 0.8 MJ x-rays, 2.6 MJ ion debris and 10 MJ neutrons. Figure 1 shows the energy spectra of the x-rays, ions and neutrons. The x-ray energy is assumed to be emitted in 20 ps, and its spectrum has a high frequency component which is the result of the Bremsstrahlung emission at electron temperatures around 40 keV during the burn. These hard x-rays will escape the xenon gas (for the base case) and penetrate deeply in the GFW. The 1.65 MeV carbon

ions carry about 66% of the 2.6 MJ ionic debris energy and can penetrate up to 3 μm in the graphite and up to 2 m in 1 torr of xenon gas.

The target is assumed to absorb 90% of the laser energy [5] and the rest (100 kJ) will be reflected and refracted from the target and is ultimately absorbed by the GFW. In the spherical geometry of SIRIUS-M, and with the assumption of uniform and normal incidence of the light on the wall, the reflected portion from one location on the wall will strike the opposite side. In effect, a train of laser pulses with rapidly attenuated amplitudes will strike the GFW.

The reflectivity of any material depends on the angle of incidence, the incident wavelength, light intensity and temperature. The optical properties of graphite as a function of all these variables are not available. A monochromatic hemispherical reflectivity of 50% has been assumed for the graphite. This value is based on data for the total hemispherical absorptivity of graphite which varies between 40% and 60% at the expected operating temperatures [6].

Figure 2 shows the incident power density on the GFW from the different sources of radiation mentioned above as a function of time and for the case of a 5 m cavity radius. The time reference point (t = 0) corresponds to the instant when the laser pulse hits the target.

3. Graphite Thermal Properties and Calculation Methods

The volumetric energy deposition rates of ions and x-rays were calculated as a function of time and distance and used together with the reflected laser light, which is assumed to be a surface heat flux due to its short wavelength. The computer code used in these calculation is ATEN [7], which is a modified and enhanced version of the two computer codes T*DAMEN [8] and A*THERMAL [9].

ATEN uses the Crank-Nicholson [10] finite difference scheme to solve the heat conduction equation. The time and space intervals in this code are varied depending on the incident radiations which differ considerably in their duration and the extent to which their energies are deposited. This allows accurate sampling of all the energy deposited in the material. Temperature-dependent properties obtained from Ref. [11] are used (Fig. 3).

The effect of the pulsed neutron irradiation on the graphite properties has not been verified and is not considered in these calculations. Although the effect of continuous neutron irradiation on these properties has been established [1], it is doubted that this effect will be the same under ICF irradiation conditions. In ICF reactors, the neutron pulse is preceded by a large temperature rise due to reflected laser light and x-rays, and followed by another temperature rise due to ions and heat flux (in the case of gas protection as will be seen later). This temperature history could have important effects on the populations of vacancies and interstitials in the materials which are the source of any change in the properties of the materials. For this reason and others [12], it is necessary to build a dedicated ICF materials test facility such as SIRIUS-M, to qualify materials for ICF reactor operations.

4. Thermal Response of Unprotected Graphite First Wall

In order to determine the minimum cavity radius corresponding to the maximum neutron wall loading for the unprotected GFW, the temperature in the first wall was calculated for different cavity radii and for different steady state temperatures. The steady state temperature is the back surface temperature (T_b) reached just before the next laser shot (rep. rate = 10 Hz). The value of this temperature depends on the method used to cool the GFW. For the

actively cooled tiles used in SIRIUS-M, T_b is approximately 500°K. Figure 4 shows the temperature rise at the front surface of the GFW for 3.5, 4.5, and 5.5 m cavity radii, and for a steady state temperature of 500°K. These results show that the surface temperature reaches its steady state value (i.e., temperature rise = zero) in approximately 1 ms, well before the next shot occurs 100 ms later. The maximum temperatures are due to the 1.65 MeV carbon ions.

The maximum temperature at the GFW front surface and the graphite evaporation rate for various steady state surface temperatures and cavity radii are shown in Figs. 5 and 6, respectively. For an evaporation limit of 1 mm per full power year (FPY), the minimum cavity radius would be 3.25 m for T_b = 500°K. This radius corresponds to 0.76 MW/m^2 neutron wall loading which is considerably less than the required goal of 2 MW/m^2 for SIRIUS-M. In addition, calculations of the GFW thermal stresses in these unprotected cases have shown that all of them are stress limited and the minimum radius is about 5.1 m. Thus, it is evident that the use of a protective scheme, such as the chamber gas in SIRIUS-M, is necessary to have high neutron wall loading and a compact design with reasonable temperatures and stresses.

5. Gas Protection

A target chamber gas can protect the first wall from the damaging effects of energetic target generated ions. The ion in the SIRIUS target with the longest range, 1.65 MeV carbon, determines the amount of gas required. For a 2 m radius target chamber, 1 torr (3.5×10^{16} cm^3) of xenon is found to stop this ion before it reaches the wall. It is assumed that the driver laser will be able to effectively transmit its energy to the target through this gas. Once the energy of the target generated x-rays and ions has been absorbed in

the xenon gas, it heats the gas to the point where it radiates this energy to the first wall. The radiated energy is absorbed on the surface of the first wall, but is spread over a much longer time than the pulse that would reach the surface if the gas were not present. The question that must be addressed is whether or not the width of the re-radiated pulse is long enough to avoid damage to the first wall.

The details of the radiation from the gas that reaches the first wall may be influenced by the design of the target. The energy of the target generated ions is roughly proportional to the target yield divided by the mass of the target. Therefore, an increase in target mass without a corresponding increase in yield leads to lower ion energies, shorter stopping lengths and higher temperatures in the gas immediately after ion deposition. Higher temperatures lead to more rapid radiation rates and possibly more damage to the surface of the wall.

A series of computer calculations has been performed to study the sensitivity of GFW damage to changes in target design. The BRICE code [13] is used to determine the stopping of ions in the gas, where the energies of the ions are scaled with the yield to mass ratio. With the equation of state data provided by the MIXERG computer code [14], temperature profiles in the gas have been calculated and are shown in Fig. 7. Results are shown for three cases: a base case, one with 42% more target mass, and one with 2.1 times the mass with the target yield held constant at 13.4 MJ. The MF-FIRE computer code [15] is then used to simulate the hydrodynamic motion and radiation transport caused by this deposition of ions and target generated x-rays. MF-FIRE has shown that most of the target generated x-rays are stopped in the gas. The time-dependent heat flux reaching the first wall as calculated by MF-FIRE is shown in Fig. 8 for the three target designs.

6. Thermal Response of Gas Protected Graphite First Wall

With a cavity radius of 2 m and 1 torr xenon, most of the ion debris and all the soft x-rays (<3 keV) could be stopped in the gas. The re-radiated heat flux from the gas together with the reflected laser light, leaked x-rays and leaked C ions at the GFW is shown in Fig. 9. The temperature rise at the front surface is shown in Fig. 10. The maximum surface temperature is 1666 K and is due to the reflected laser light from the target. The evaporation rate of the GFW is insignificant. With the elimination of most of the direct energy deposition from the ions by use of the xenon cavity gas, the reflected laser light from the target becomes the decisive element in determining the cavity size.

7. Stress Analysis of First Wall

The chamber gas will transmit a shock pressure to the first wall after each microexplosion. The resulting dynamic stresses have been determined for the case in which the structure is represented by a thin spherical shell. The pressure histories of the three target designs are shown in Fig. 11. The base case corresponds to an impulse of 4.80 Pa-s. The impulse values for the other two cases are essentially the same because the higher pressures are accompanied by shorter effective pulse widths. Results of the mechanical analysis indicate that the peak tensile stress in the graphite is 1.52 MPa, which is only 10.6% of the tensile strength, 14.38 MPa, at 500°K [1].

Energy deposition in the first wall will develop an intense compressive thermal stress distribution at the inner surface. Since the heated layer is comparatively very thin it will be almost totally constrained by the unaffected graphite. The first surface thermal stress history is shown in Fig. 12. The maximum value is 61.37 MPa occurring at 17.7 ns, and is 87.6% of the compressive strength (70.06 MPa).

8. Conclusions

Thermal and stress analyses of the graphite first wall in SIRIUS-M have been presented; all the cases considered are stress-limited. The use of gas protection is necessary to avoid the direct energy deposition of x-rays and ions which produce the highest temperature rise in the first wall. The absorbed energy in the gas is re-radiated in a longer time which results in a much smaller heat flux to the first wall. In this case (i.e., gas protected), the reflected laser light produces the largest temperature rise.

Acknowledgment

Support for this work has been provided by the U.S. Department of Energy.

References

[1] G.R. Hopkins, R.J. Price, R.E. Bullock, J.A. Dalessandro, and N.B. Elsner, "Carbon and Silicon Carbide As First Wall Materials In Inertial Confinement Fusion Reactors," Genera Atomic Report Number GA-A14894 (1978).

[2] R.W. Conn et al., "SOLASE, A Laser Fusion Reactor Study," University of Wisconsin Fusion Technology Institute Report UWFDM-220 (1977).

[3] B. Badger et al., "SIRIUS-M: A Symmetric Illumination, Inertially Confined Direct Drive Materials Test Facility," University of Wisconsin Fusion Technology Institute Report UWFDM-651 (1985).

[4] S.I. Abdel-Khalik et al., "SIRIUS-M: A Symmetric Illumination, Inertially Confined Direct Drive Materials Test Facility," J. Nucl Mater. 00 (1986) 0.

[5] R.S. Craxton and R.L. McCrory, UR LLE, Report No. 108 (1980).

[6] R. Siegel and J.R. Howell, "Thermal Radiation Heat Transfer," McGraw-Hill Book Company, New York, (1972).

[7] H. Attaya, to be published.

[8] T.O. Hunter and G.L. Kulcinski, "T*DAMEN, A Computer Code For Transient Radiation Damage Analysis," University of Wisconsin Fusion Technology Institute Report UWFDM-247 (1978).

[9] A. Hassanien, "Thermal Effects and Erosion Rates Resulting from Intense Deposition of Energy in Fusion Reactor First Walls," University of Wisconsin Fusion Technology Institute Report UWFDM-465 (1982).

[10] R.D. Richtmeyer and K.W. Morton,"Difference Methods for Initial Value Problems," Interscience Publishers, Inc., New York, (1965).

[11] N.S. Rasor and J.D. McClelland, "Thermal Properties of Graphite, Molybdenum and Tantalum to Their Destruction Temperatures," J. Phys. Chem. Solids, 15 (1960) 17.

[12] G.L. Kulcinski and M.E. Sawan, "Differences Between Damage in Inertial and Magnetic Confinement Materials Test Facilities," J. Nucl. Mater. 133 & 134 (1985) 52.

[13] D.K. Brice, "Three-Parameter Formula for the Electronic Stopping Cross Section at Non-Relativistic Velocities," Phys. Rev. A 6, 1791 (1972).

[14] R.R. Peterson and G.A. Moses, "MIXERG - An Equation of State and Opacity Computer Code," Computer Phys. Comm. 28, 367 (1983).

[15] G.A. Moses, R.R. Peterson, and T.J. McCarville, "MF-FIRE - A Multi-frequency Radiative Transfer Hydrodynamics Code," Computer Phys. Comm. 36, 249 (1985).

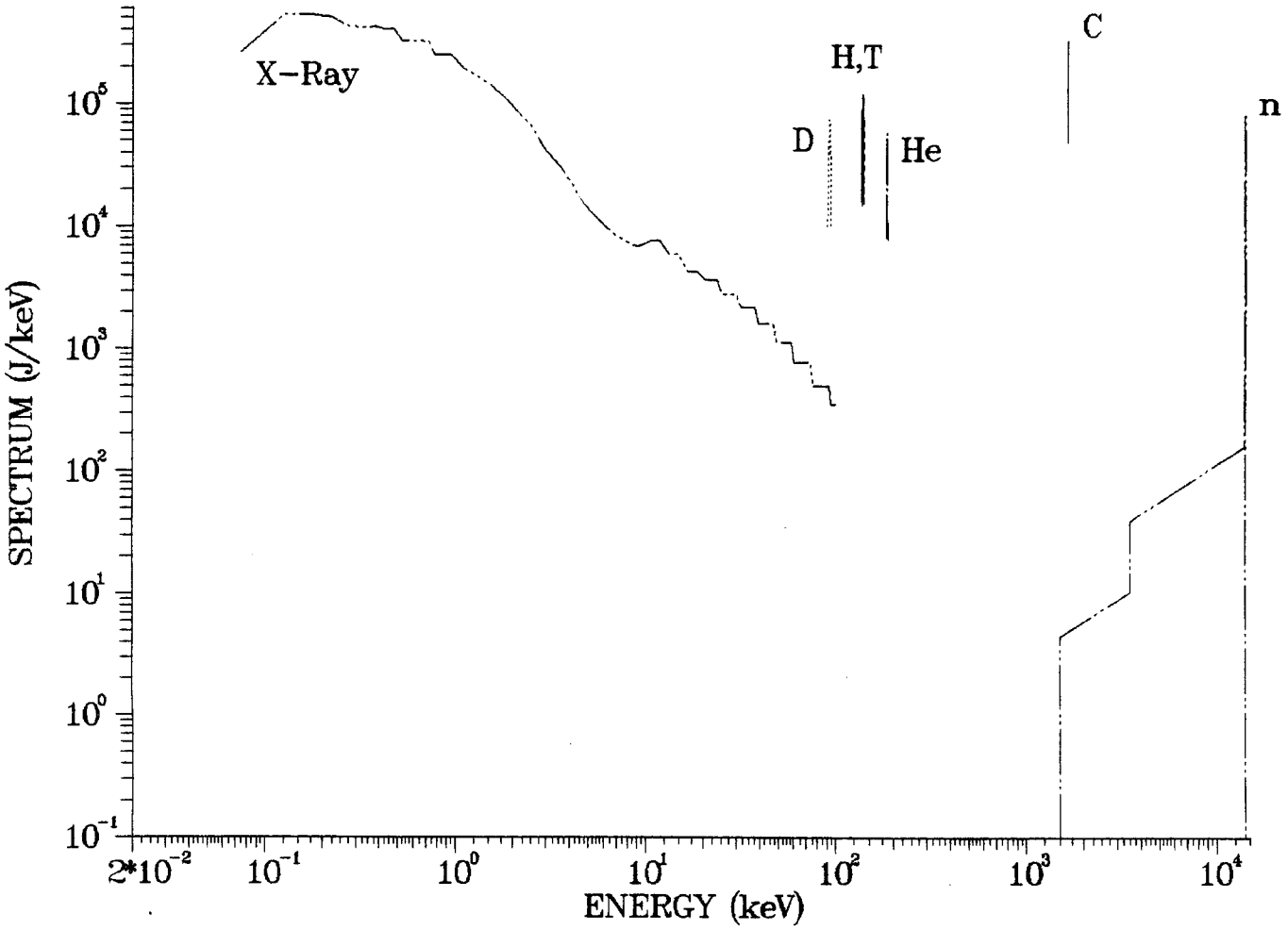

Fig. 1. X-ray, ion, and neutron spectra.

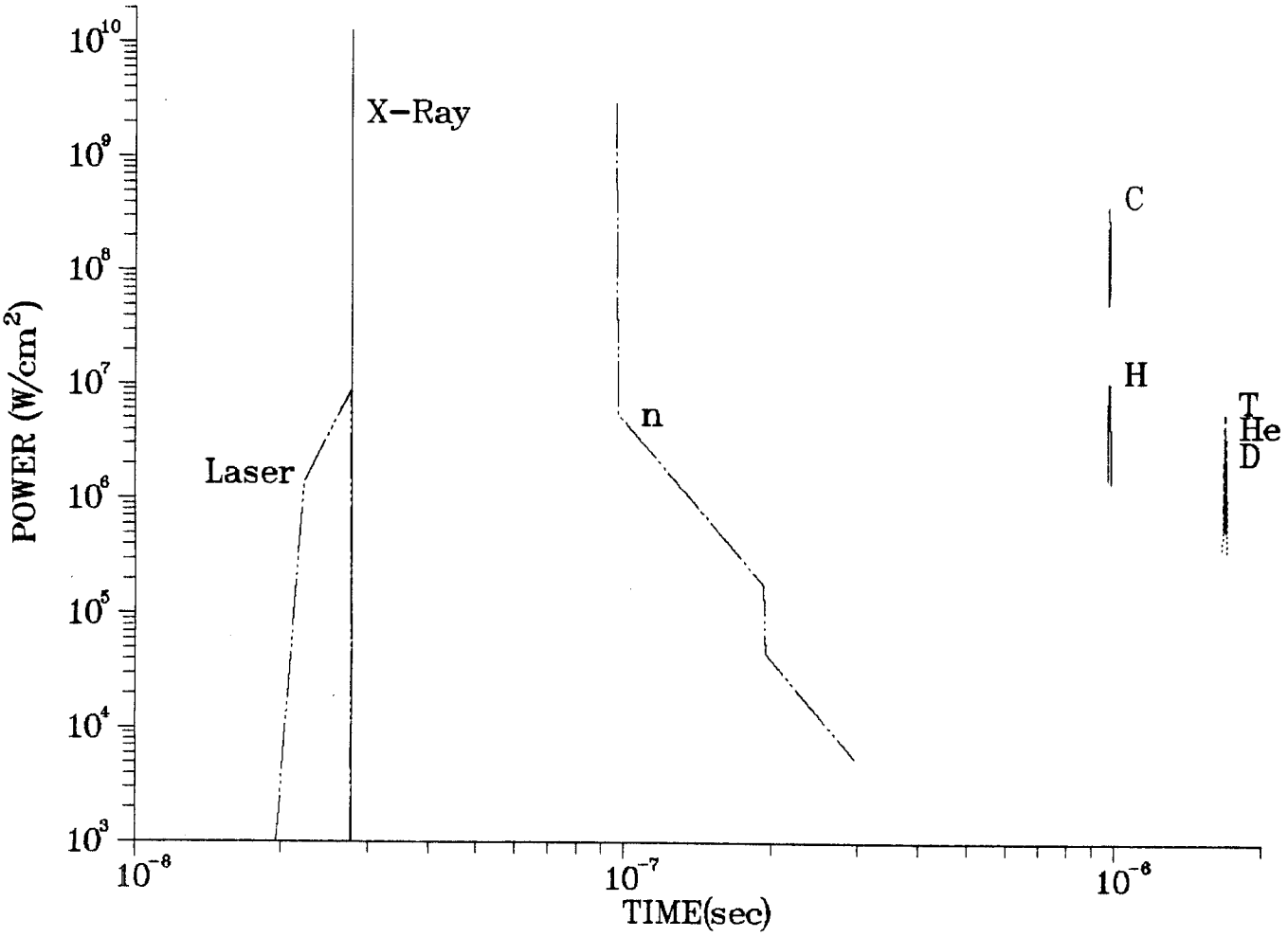

Fig. 2. Incident power on an unprotected wall (R = 5 m) due to x-rays, ions, neutrons and laser light reflected from the target.

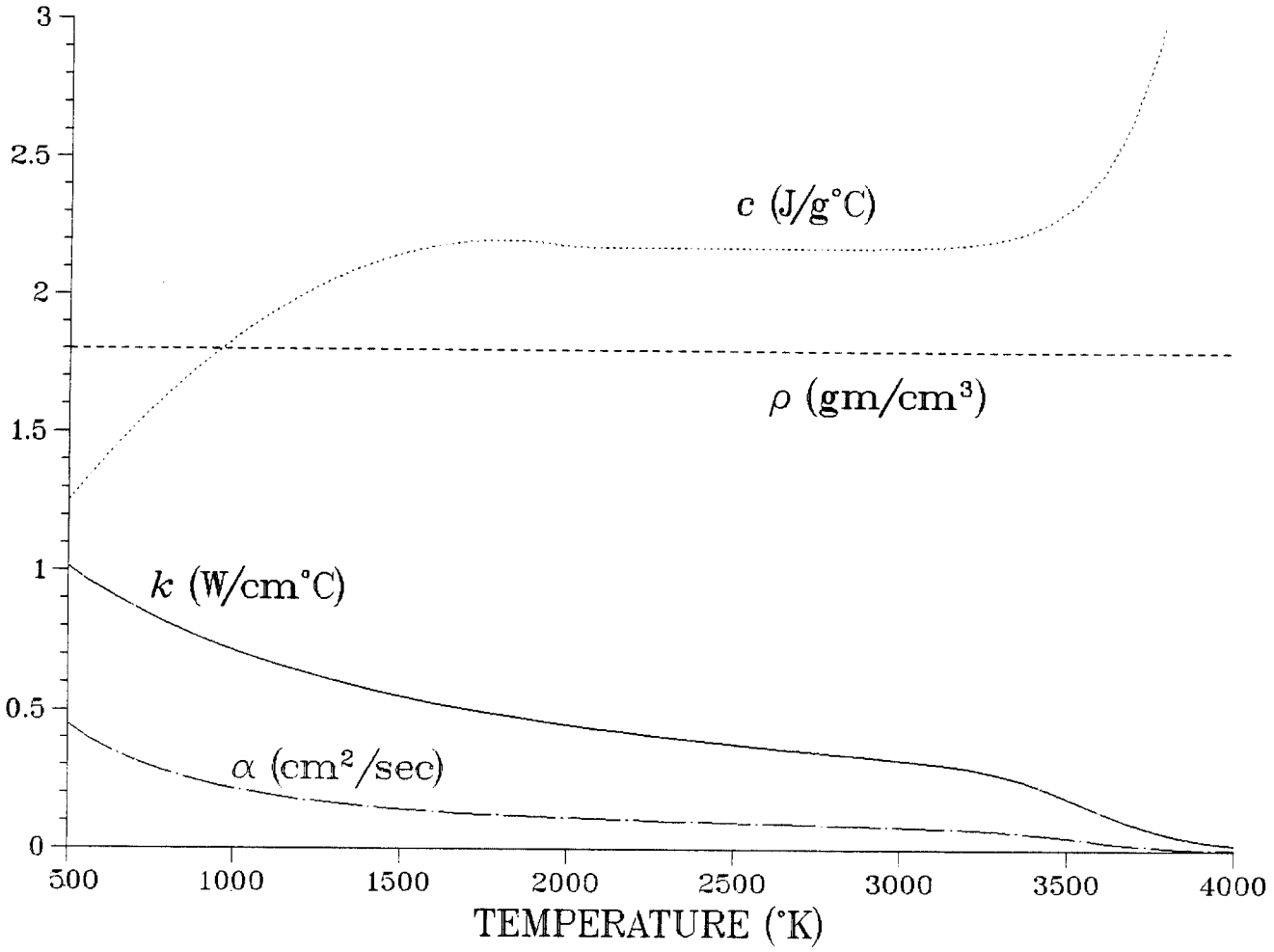

Fig. 3. Graphite thermal properties as a function of temperature: density ρ, conductivity k, diffusivity α, specific heat c.

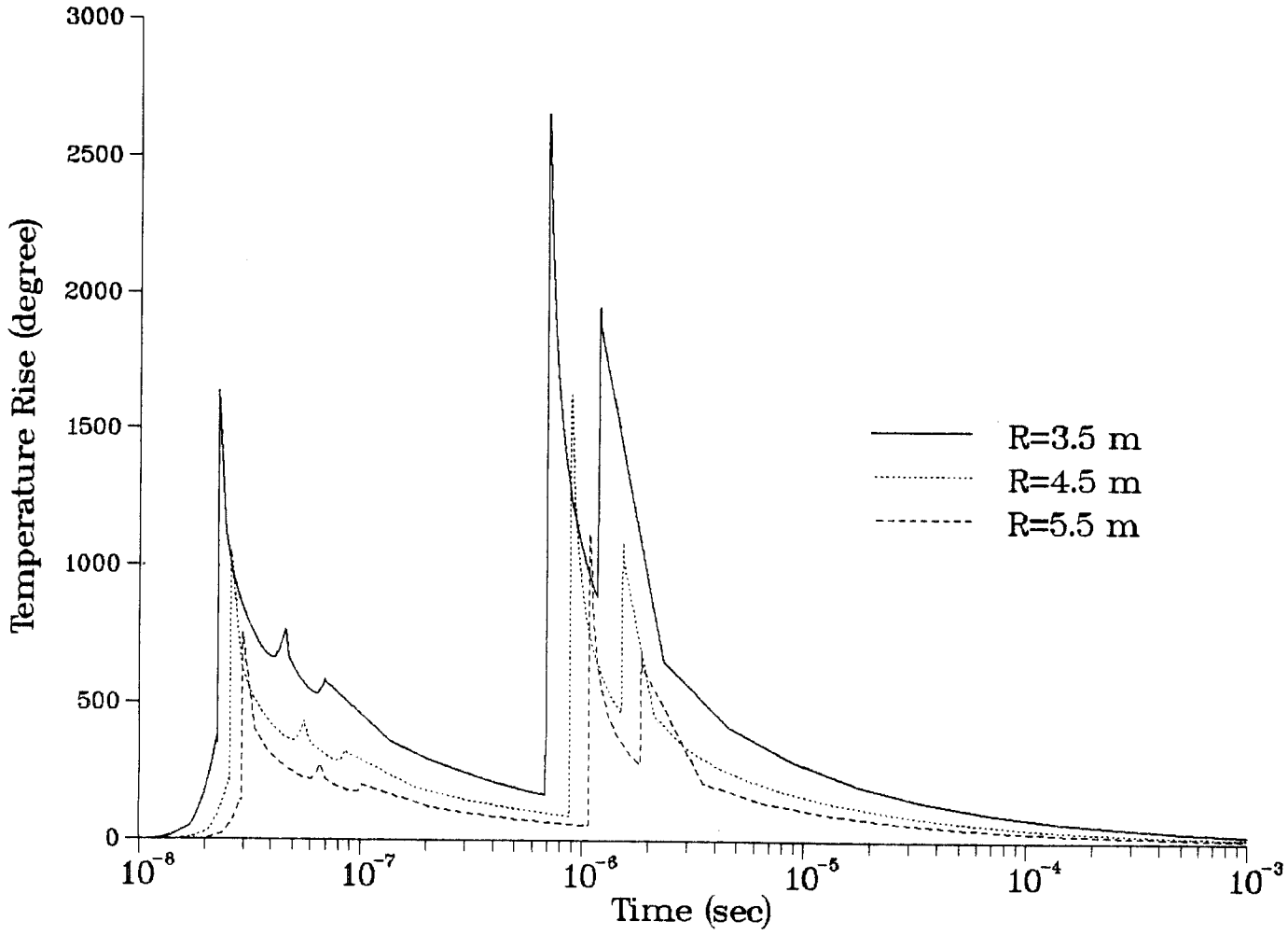

Fig. 4. Temperature rise at the graphite first wall front surface for cavity radii of 3.5, 4.5 and 5.5 m, with a steady state temperature of 500°K.

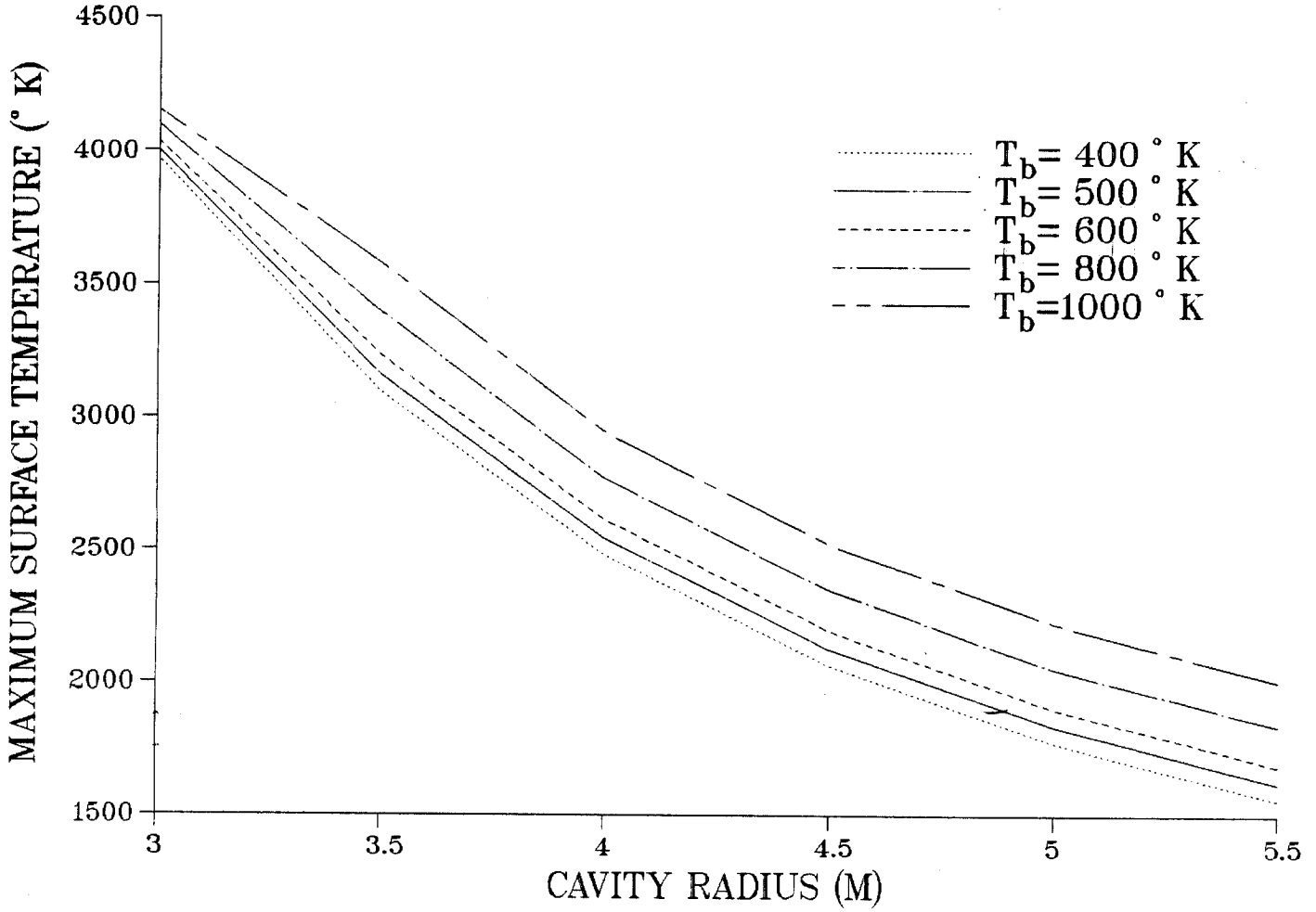

Fig. 5. The maximum surface temperature for various steady state temperatures and cavity radii.

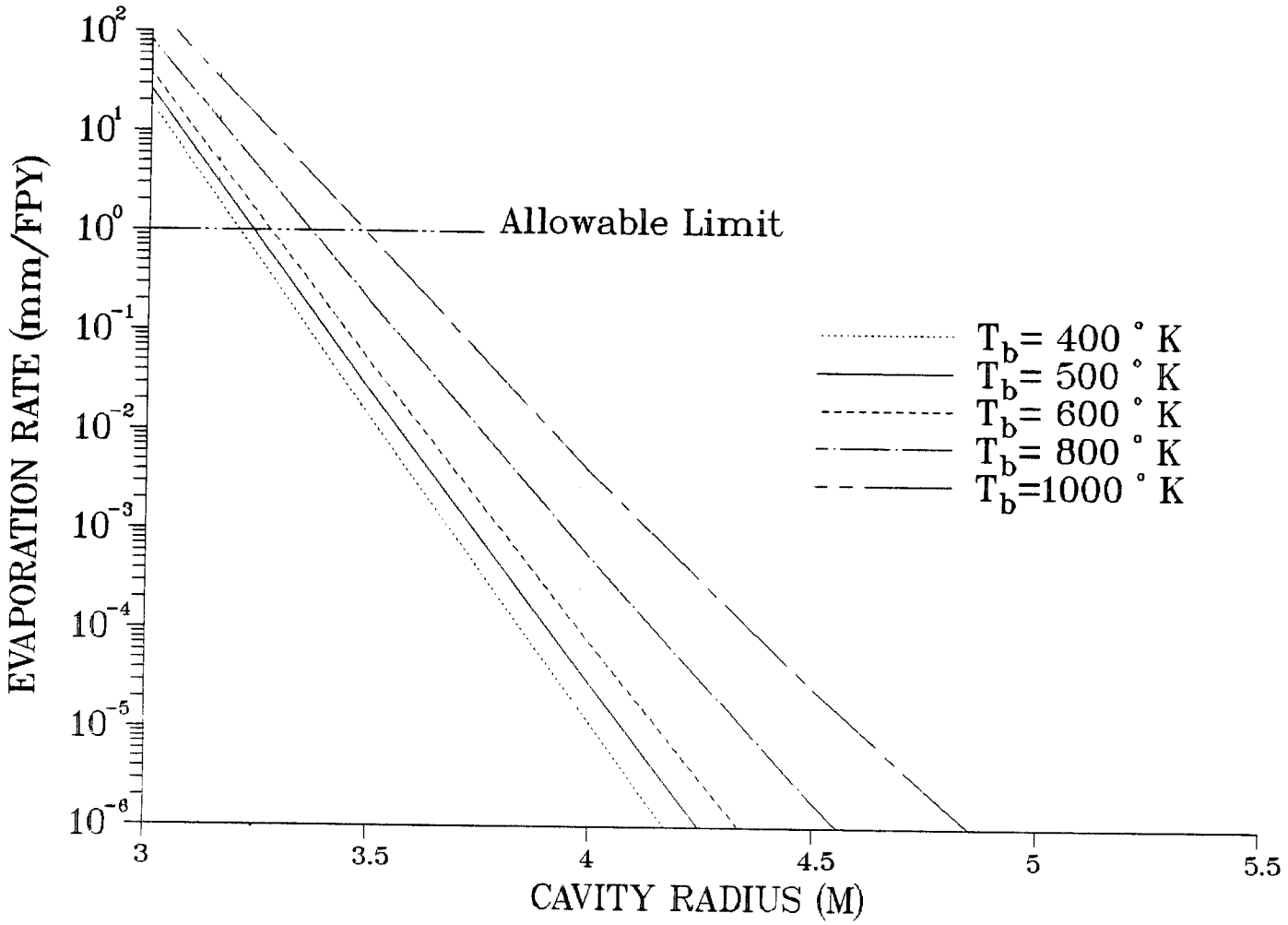

Fig. 6. Evaporation rate as a function of the cavity radius and steady state surface temperature.

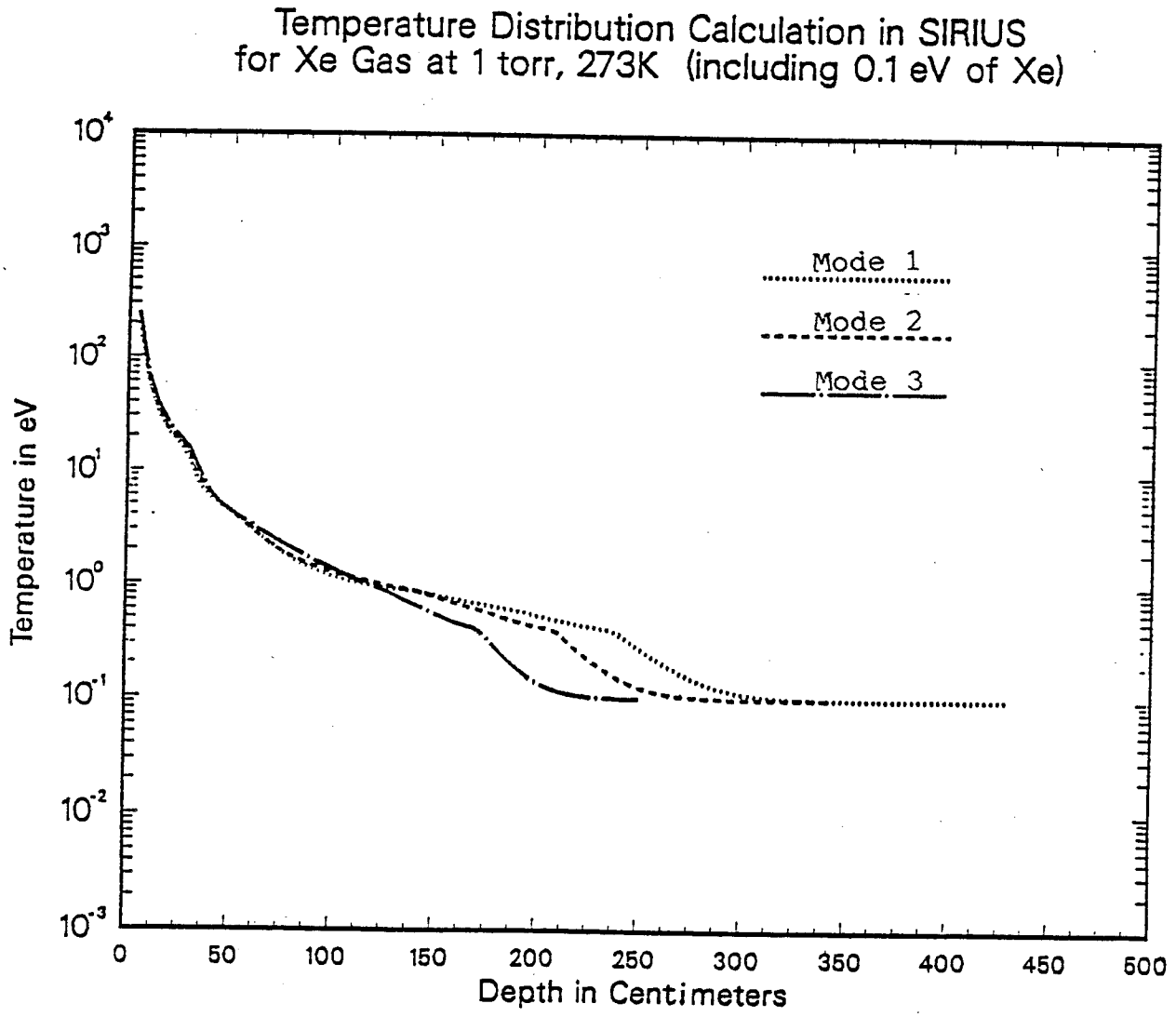

Fig. 7. Temperature rise in Xe gas due to energy deposition of ions.

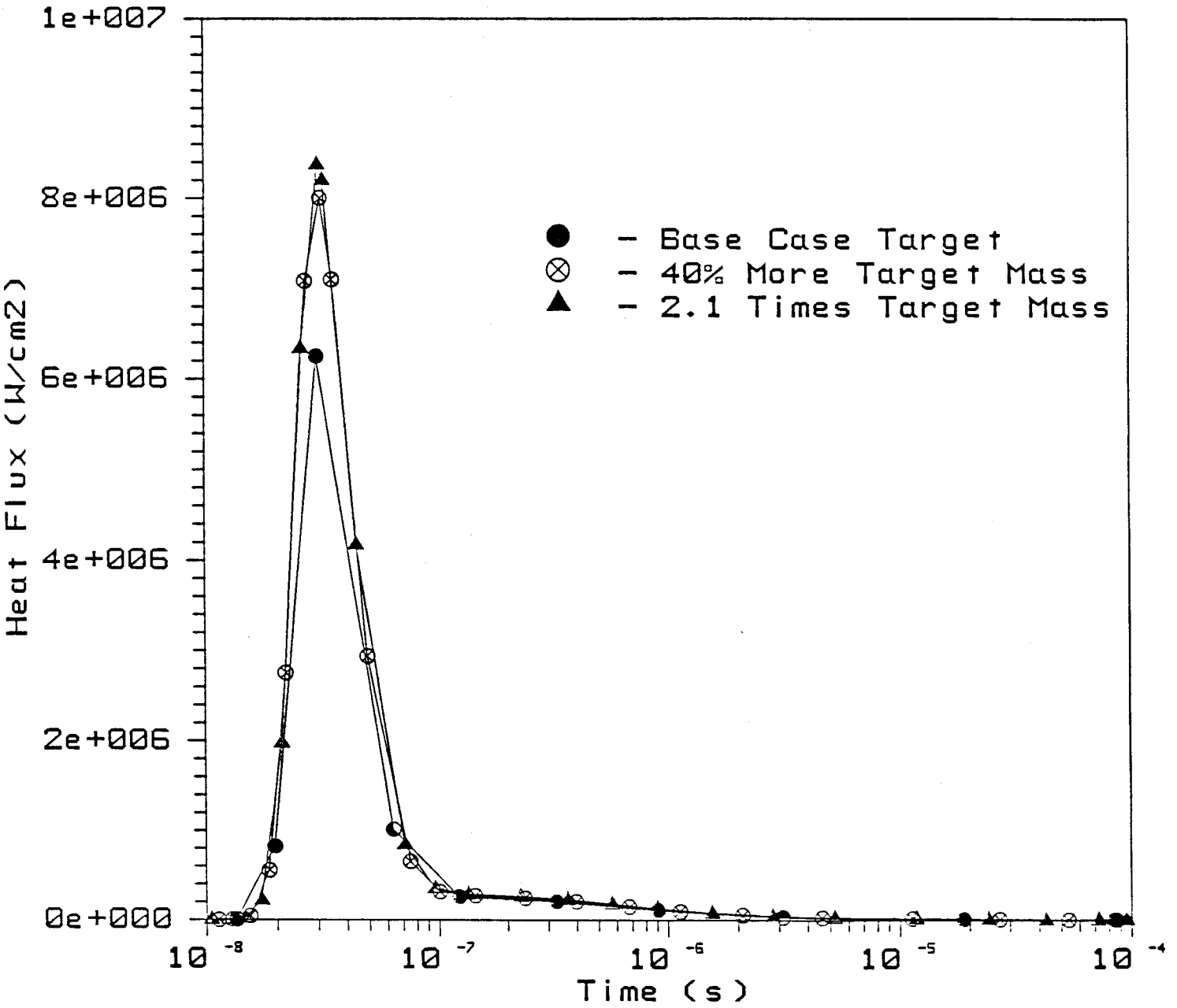

Fig. 8. Graphite first wall heat flux for various target designs.

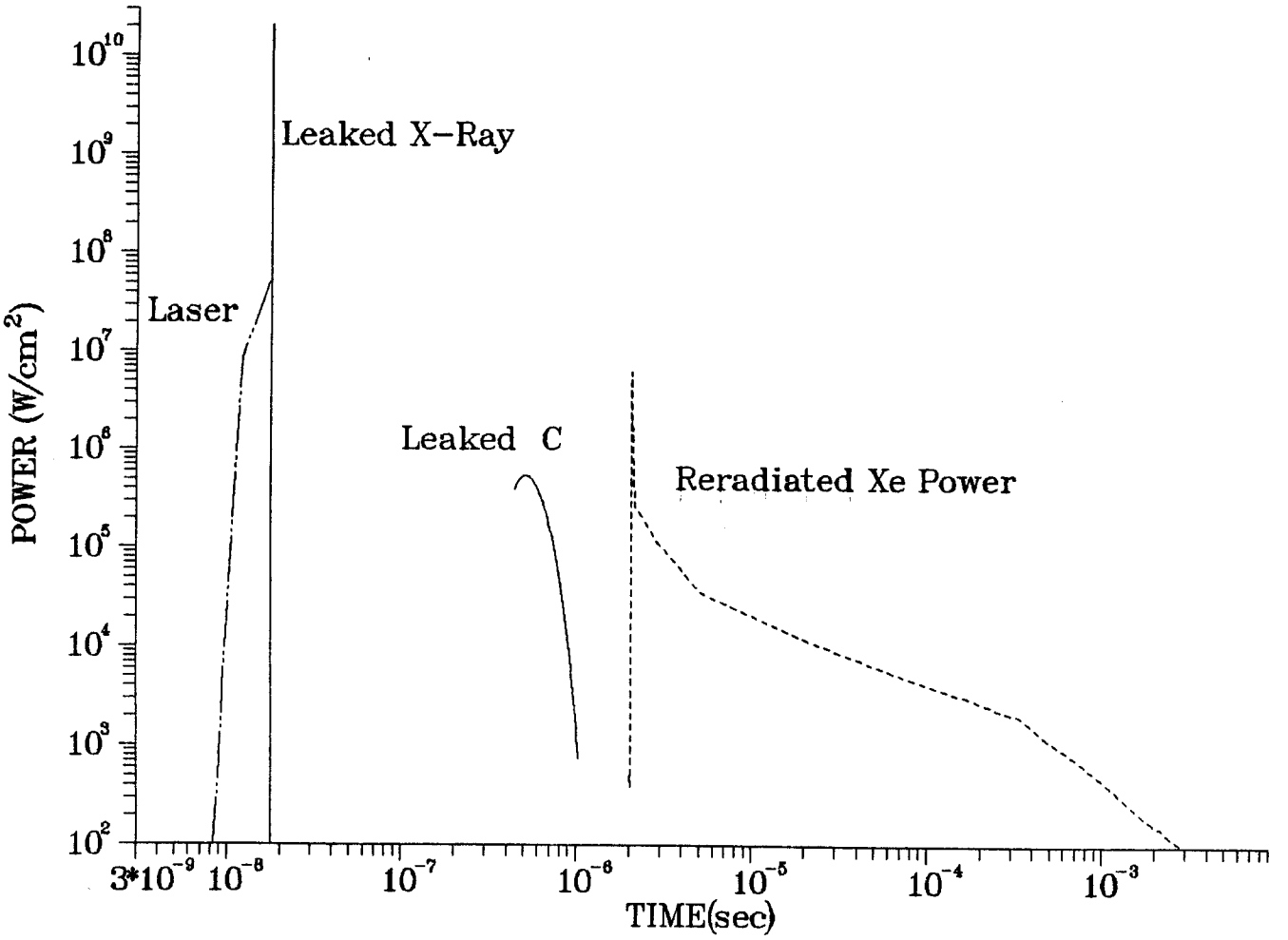

Fig. 9. Total heat flux on first wall including reflected laser, re-radiated, and unabsorbed target x-rays and ions for base case.

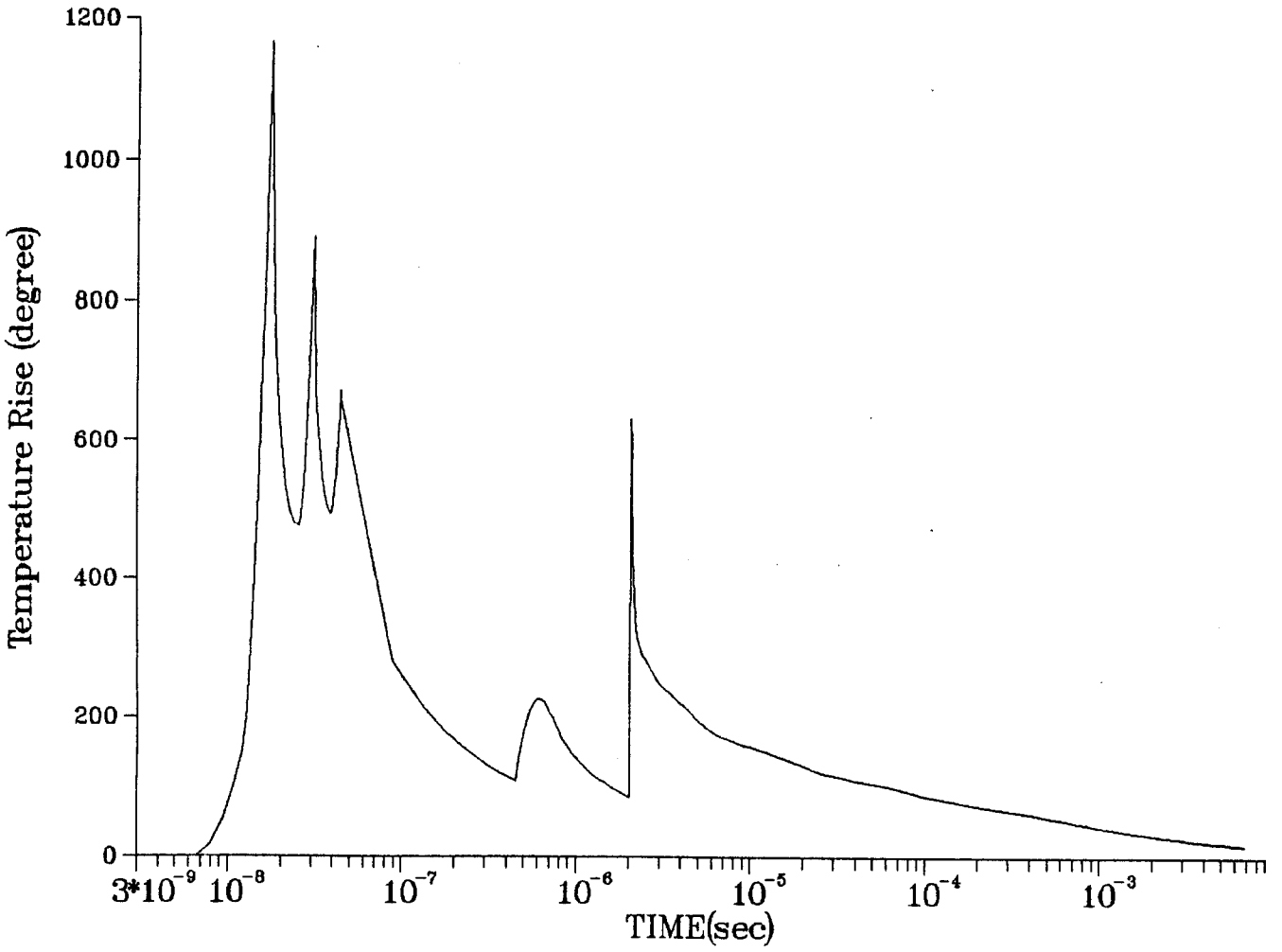

Fig. 10. Temperature rise in graphite first wall of SIRIUS-M base case.

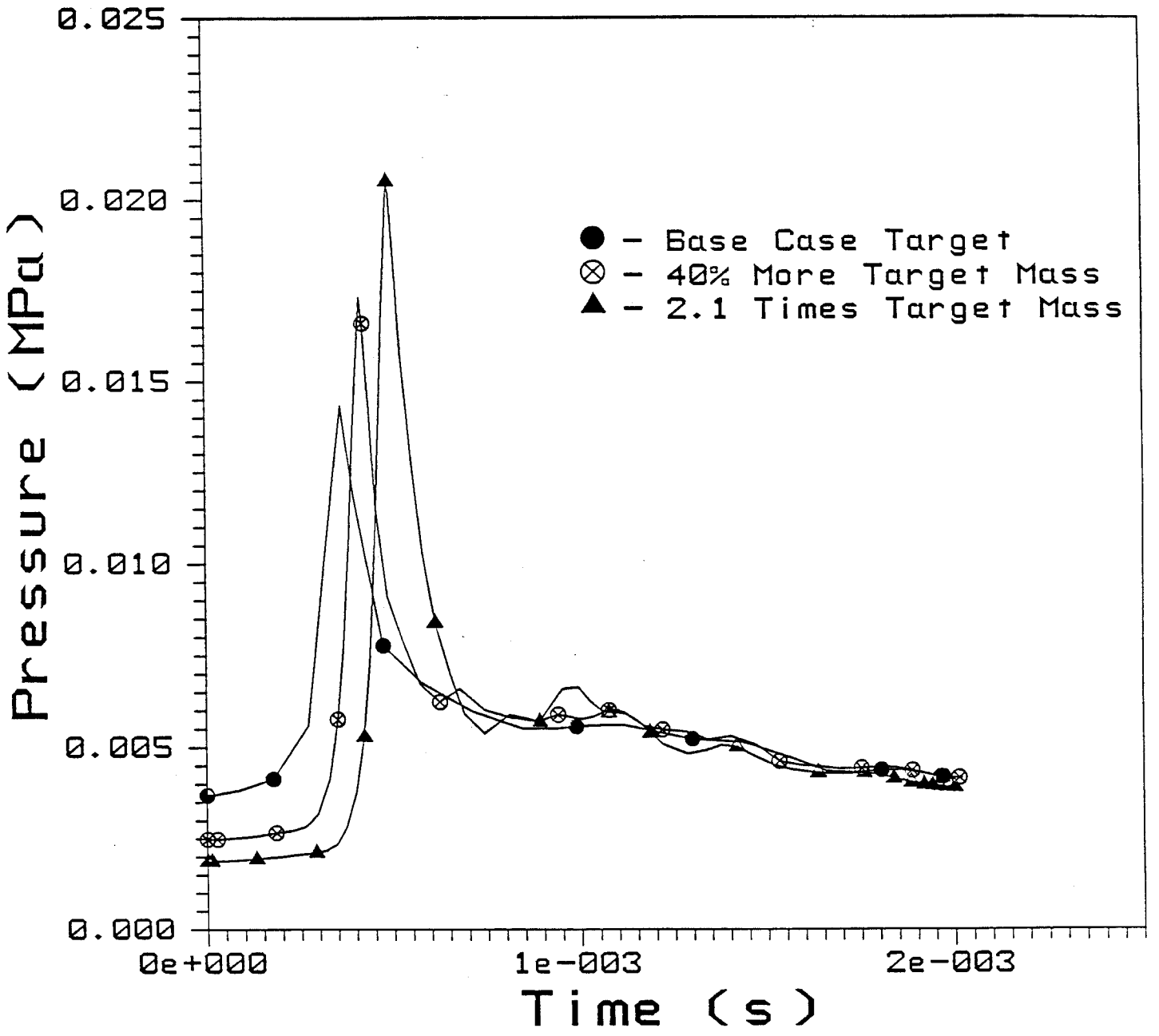

Fig. 11. Stagnation pressure on the first wall.

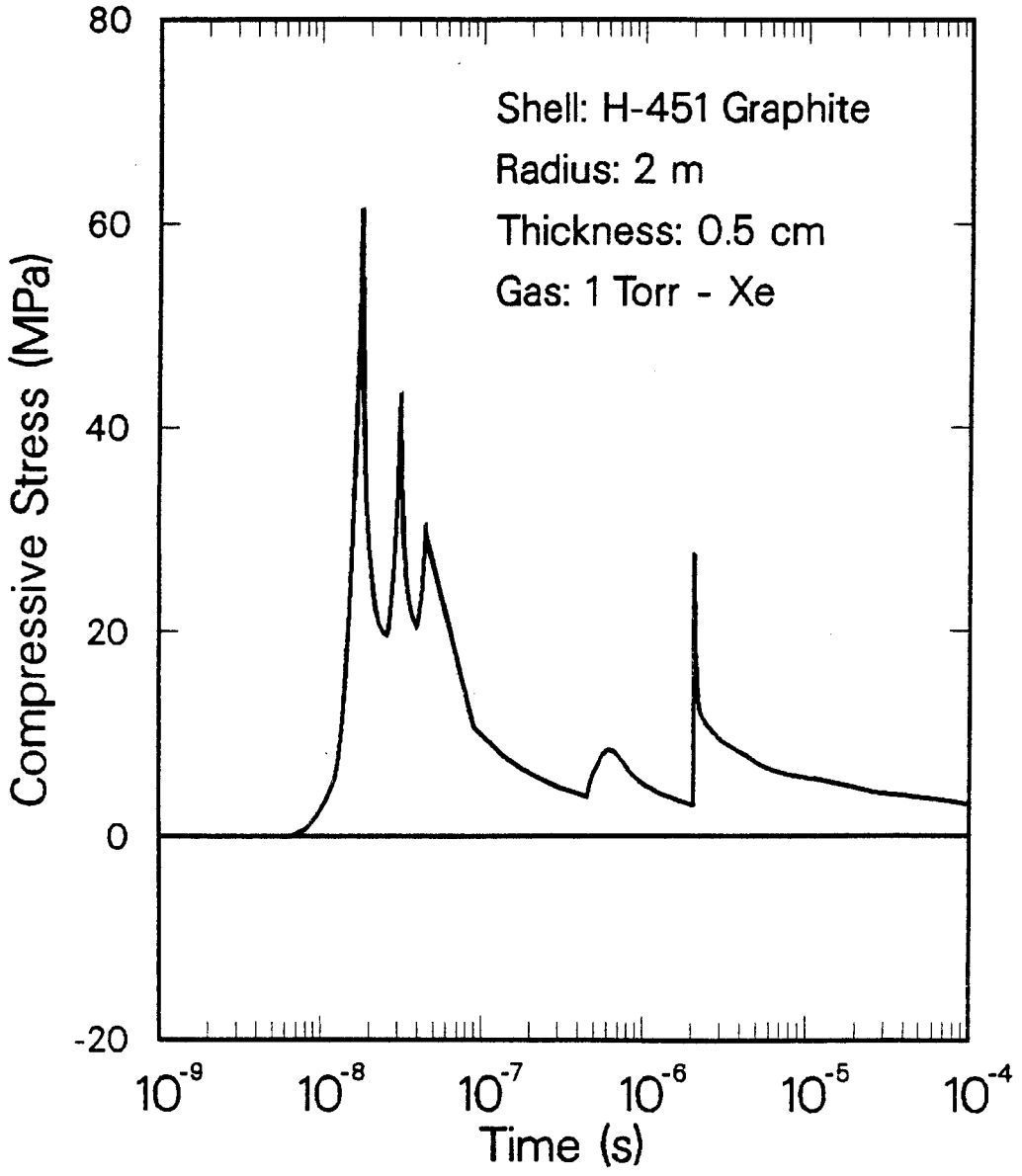

Fig. 12. SIRIUS-M graphite first wall thermal stress history.